Analisi Numerica. – *A computational approach to fractures in crystal growth.* Nota di MATTEO NOVAGA ed EMANUELE PAOLINI.

ABSTRACT. – In the present paper, we motivate and describe a numerical approach in order to detect the creation of fractures in a facet of a crystal evolving by anisotropic mean curvature. The result appears to be in accordance with the known examples of facet-breaking. Graphical simulations are included.

KEY WORDS: Nonlinear partial differential equations of parabolic type; Crystal growth; Non-smooth analysis.

RIASSUNTO. – *Un approccio numerico alle fratture nella crescita di cristalli.* In questo lavoro, presentiamo e discutiamo un approccio numerico al problema di individuare la nascita di fratture in una faccia di un cristallo che si evolve per curvatura media anisotropa. I risultati sono in accordo con gli esempi noti fino ad ora di frattura di facce. Sono inoltre incluse alcune simulazioni grafiche.

0. INTRODUCTION

We model crystal growth in $\mathbb{R}^3$ as an anisotropic evolution by mean curvature when the ambient space is endowed with a convex one-homogeneous function whose unit ball (usually called the Wulff shape) is a polyhedron. Such evolutions are considered in materials science and phase transitions when the velocity of the evolving front depends on the orientation of the normal vector and has a finite number of preferred directions. This problem has been widely studied; we refer among others to [10], [12], [7], [9], [3].

This motion has a variational interpretation as "gradient flow" of an associated crystalline energy defined on the subsets of $\mathbb{R}^3$ having finite perimeter, see [12], [2] and Remark 1.2 below.

The simplest situation of motion by crystalline curvature is the bidimensional case. In this case short time existence and uniqueness of the evolution has been established, as well as an inclusion principle between the evolving fronts. Moreover, if the initial set E is a polygon compatible with the Wulff shape, its edges translate parallely to themselves during the evolution, so that no edge–breaking occurs [10], [12], [1]. It is interesting to observe that the situation becomes quite different in presence of a space dependent forcing term [8], since new edges may create during the evolution.

In the three–dimensional case, facet–breaking phenomena are quite common and, even starting from a polyhedral set whose shape is very close to the Wulff shape, some facets can break or bend and curve portions of the boundary can appear (see [4], [11], [13] for related examples). For what concerns the qualitative behaviour of the evolving interfaces, to the best knowledge of the authors, the problem of understanding if and where facet–breaking phenomena take place has not a definite answer.

Here we try to answer to this question by means of a numerical approach. More precisely, with a formal argument we show that the crystalline curvature of an evolving set (which is equal to the velocity) is expected to solve a minimum problem on each facet.

This corresponds to look for the canonical element of the subdifferential of the crystalline energy (restricted to the facet), which is a common procedure in multivalued convex analysis (compare [9]). We then determine this minimum with a numerical approach, using a finite element method. The discontinuities of the crystalline curvature correspond to the fractures appearing in the facet, more precisely the facet will not break or bend if and only if the crystalline curvature is constant on the facet.

The plan of the paper is the following. In Section 1 we give some notation and we recall, following [3], the general definitions of ϕ-regular set and ϕ-regular flow. Observe that these definitions concern Lipschitz surfaces, and we do not restrict ourselves to polyhedral surfaces in view of the examples discussed in Section 3. We also introduce the minimum problem (5), which we will solve numerically, in order to characterize the velocity of the evolving set. In Section 2 we present the algorithm which we use to find such a minimum, and in Section 3 we discuss the results of the algorithm applied to the examples of [4]. Numerical simulation are in accordance with the result of [4].

More graphics and the source code of the program (written in C++ language) are available on `http://rock.sns.it/crystals/`.

We thank G. Bellettini and M. Paolini for many useful discussions.

1. Notation and main definitions

In the following we denote by $\cdot$ the standard euclidean scalar product in $\mathbb{R}^3$, and by $|\cdot|$ the euclidean norm of $\mathbb{R}^3$. Given a subset A of $\mathbb{R}$ or

$\mathbb{R}^2$, we denote by $|A|$ the Lebesgue measure of A. $\mathcal{H}^k$, $k = 1, 2, 3$ will denote the k-dimensional Hausdorff measure.

We indicate by $\phi : \mathbb{R}^3 \to [0, +\infty[$ a convex function satisfying the properties

$$\phi(\xi) \geq \Lambda|\xi|, \qquad \phi(a\xi) = a\phi(\xi), \qquad \xi \in \mathbb{R}^3,\ a \geq 0, \tag{1}$$

for a suitable constant $\Lambda \in]0, +\infty[$, and by $\phi^o : \mathbb{R}^3 \to [0, +\infty[$, $\phi^o(\xi^*) := \sup\{\xi^* \cdot \xi \ : \ \phi(\xi) \leq 1\}$ the dual of ϕ. We set

$$\mathcal{F}_\phi := \{\xi^* \in \mathbb{R}^3 : \phi^o(\xi^*) \leq 1\}, \qquad \mathcal{W}_\phi := \{\xi \in \mathbb{R}^3 : \phi(\xi) \leq 1\}.$$

$\mathcal{F}_\phi$ and $\mathcal{W}_\phi$ are convex sets whose interior parts contain the origin. In this paper we shall assume that ϕ is crystalline, i.e. $\mathcal{W}_\phi$ (and hence $\mathcal{F}_\phi$) is a convex polyhedron. $\mathcal{F}_\phi$ is usually called the Frank diagram and $\mathcal{W}_\phi$ the Wulff shape.

Let $T^o : \mathbb{R}^3 \to \mathcal{P}(\mathbb{R}^3)$ be the duality mapping defined by

$$T^o(\xi^*) := \frac{1}{2}\partial^-(\phi^o(\xi^*))^2, \qquad \xi^* \in \mathbb{R}^3,$$

where $\mathcal{P}(\mathbb{R}^3)$ is the class of all subsets of $\mathbb{R}^3$ and ∂^- denotes the subdifferential in the sense of convex analysis. T^o is a multivalued maximal monotone operator, and

$$T^o(a\xi^*) = aT^o(\xi^*), \qquad a \geq 0.$$

One can show that

$$\xi^* \cdot \xi = \phi^o(\xi^*)^2 = \phi(\xi)^2, \qquad \xi^* \in \mathbb{R}^3,\ \xi \in T^o(\xi^*).$$

Given $E \subset \mathbb{R}^3$ and $x \in \Omega$, we set

$$\mathrm{dist}_\phi(x, E) := \inf_{y \in E} \phi(x - y), \qquad \mathrm{dist}_\phi(E, x) := \inf_{y \in E} \phi(y - x),$$

$$d^E_\phi(x) := \mathrm{dist}_\phi(x, E) - \mathrm{dist}_\phi(\mathbb{R}^3 \setminus E, x).$$

At each point where d^E_ϕ is differentiable, there holds [5]

$$\phi^o(\nabla d^E_\phi) = 1.$$

The next definition generalizes to the crystalline case the notion of smooth surface [4].

Definition 1.1. *Let* $E \subset \mathbb{R}^3$ *and* $n_\phi : \partial E \to \mathbb{R}^3$ *be Borel–measurable. We say that the pair* (E, n_ϕ) *is* ϕ*-regular if*

1. *the set* ∂E *is compact and Lipschitz continuous;*

2. $$n_\phi(x) \in T^o\left(\nabla d_\phi^E(x)\right) \qquad \mathcal{H}^2 - a.e.\ x \in \partial E;$$

3. *there is an open set* $A \supseteq \partial E$ *such that for a.e.* $y \in A$ *there exists a unique* $(x,s) \in \partial E \times \mathbb{R}$ *so that* $y = x + s n_\phi(x)$ *and letting* $n_\phi^e(y) := n_\phi(x)$ *there holds*
$$n_\phi^e \in L^\infty(A; \mathbb{R}^3), \qquad \mathrm{div} n_\phi^e \in L^\infty(A);$$

4. $\mathrm{div} n_\phi^e$ *admits a trace on* ∂E*, which we denote by* $\mathrm{div}_\tau n_\phi \in L^\infty(\partial E)$.

We say that E *is* ϕ*-regular if there exists a function* $n_\phi : \partial E \to \mathbb{R}^3$ *such that* (E, n_ϕ) *is a* ϕ*-regular pair.*

Such a generality (as in Definition 1.4 below) is needed in view of the second example of Section 3 (see also Remark 1.5 below). We notice that, if ∂E is a plane, then div_τ is the usual tangential divergence in the sense of distributions.

In the crystalline literature n_ϕ is usually called the Cahn-Hoffman vector field. Given a ϕ-regular pair (E, n_ϕ), we define the ϕ-mean curvature κ_ϕ of ∂E at $\mathcal{H}^2$-almost every $x \in \partial E$ as

$$\kappa_\phi := \mathrm{div}_\tau\, n_\phi. \tag{2}$$

Remark 1.2. *We observe that the vector field* $-\kappa_\phi\, n_\phi$ *in Definition 1.1 has a variational interpretation as "gradient flow" of the crystalline energy*

$$A \to \int_{\partial A} \phi^o(\nu_A) d\mathcal{H}^2,$$

where ν_A *is the exterior unit normal to* ∂A*, see [4] for a formal computation in this direction.*

Remark 1.3. *Let* E *be a polyhedral set having the following property: given any vertex* v *of* ∂E*, the intersection of* $T^o(\nabla d_\phi^E)_{|Q}$ *over all facets* Q *containing* v *is non empty. Then there exists a vector field* $n_\phi \in \mathrm{Lip}(\partial E; \mathbb{R}^3)$ *such that* (E, n_ϕ) *is a* ϕ*-regular pair.*

Evolution law.

If $t \in [0,T] \mapsto E(t) \subset \mathbb{R}^3$ is a parametrized family of subsets of $\mathbb{R}^3$, we let

$$d_\phi^{E(t)}(x) := \mathrm{dist}_\phi(x, E(t)) - \mathrm{dist}_\phi(\mathbb{R}^3 \setminus E(t), x).$$

Whenever no confusion is possible, we set $d_\phi(x,t) := d_\phi^{E(t)}(x)$.

We now define a ϕ-regular flow $(E(t), n_\phi(\cdot,t))$, for $t \in [0,T]$, as a ϕ-regular evolution of a boundary moving with velocity, in the n_ϕ-direction, equal to $-\kappa_\phi$ (see [4]).

Definition 1.4. *A ϕ-regular flow is a pair $(E(t), n_\phi(\cdot,t))$, $n_\phi(\cdot,t) : \partial E(t) \to \mathbb{R}^3$, which satisfies the following properties:*

(1) $(E(t), n_\phi(\cdot,t))$ is ϕ-regular for any $t \in [0,T]$;

(2) the function d_ϕ is Lipschitz continuous on $\mathbb{R}^3 \times [0,T]$, differentiable for a.e. $t \in [0,T]$ and for $\mathcal{H}^2-$ a.e. $x \in \partial E(t)$, and such that

$$\frac{\partial d_\phi}{\partial t}(x,t) = \kappa_\phi(x,t), \qquad a.e.\ \ t \in [0,T],\ \mathcal{H}^2 - a.e.\ x \in \partial E(t). \quad (3)$$

In case no new facet creates, the previous evolution law concides with the evolution law considered in [12] and [9].

Remark 1.5. *We observe that the class of polyhedral subsets of $\mathbb{R}^3$ seems not to be stable under the evolution defined by (3), i.e. some polyhedral set may develop curve portions of the boundary during the evolution (see [4], [11], [13] and Section 3 below).*

Let now (E, n_ϕ) be a ϕ-regular pair. Assume that E is a polyhedron and let F be a facet of ∂E. We notice that by [9, Lemma 9.2], the trace of $n_\phi \cdot \nu_F$ is well–defined in $L^\infty(\partial F)$ (ν_F is the exterior unit normal to ∂F lying in the plane containing by F). For $\mathcal{H}^1$-a.e. $s \in \partial F$, we denote such a trace by $c_F(s)$. Let also

$$v_F := \frac{1}{|F|}\int_{\partial F} c_F(s)\ \mathrm{d}\mathcal{H}^1(s) = \frac{1}{|F|}\int_F \kappa_\phi(x)\ \mathrm{d}\mathcal{H}^2(x).$$

Notice that, since the facet F is planar, for any $x \in \mathrm{int}(F)$ it is well–defined the convex set $T^o(\nabla d_\phi^E(x)) \subset \partial \mathcal{W}_\phi$, and it is independent of $x \in \mathrm{int}(F)$.

Using [9, Lemma 9.2], one can get the following result (see also [13]).

Proposition 1.6. *Let E be a ϕ-regular polyhedron, and F be a facet of ∂E. Then, the function $c_F \in L^\infty(\partial F)$ depends only on E and is independent of the choice of n_ϕ. More precisely, for $\mathcal{H}^1$-a.e. $s \in \partial F$ there holds*

$$c_F(s) = \begin{cases} \sup \{n \cdot \nu_F(s) : \ n \in T^o(\nabla d_\phi^E)\} \text{ if } E \text{ is locally convex in } s, \\ \inf \{n \cdot \nu_F(s) : \ n \in T^o(\nabla d_\phi^E)\} \text{ if } E \text{ is locally concave in } s. \end{cases} \tag{4}$$

Observe that expression (4) is in agreement with the corresponding definition given in [12].

We now try to characterize the crystalline curvature defined in (2) as minimum of a variational problem. This formal argument is intended to motivate the numerical approach discussed in Section 2.

Let $(E(t), n_\phi(\cdot,t))$, $t \in [0,\tau]$, be a ϕ-regular flow, and assume for simplicity that $E := E(0)$ is a polyhedron. Then we expect that $n_\phi(\cdot,0)$ solves the following minimum problem on ∂E

$$\begin{aligned} \min \ \Big\{ \int_{\partial E} \big(\mathrm{div}_\tau \ \xi\big)^2 \phi^o(\nu_E) \ \mathrm{d}\mathcal{H}^2(x) : \ \xi \in L^\infty(\partial E; \mathbb{R}^3), \\ \mathrm{div}_\tau \ \xi \in L^2(\partial E), \ \xi \in T^o(\nabla d_\phi^E) \ \mathcal{H}^2 - a.e. \text{ on } \partial E \Big\}. \end{aligned} \tag{5}$$

Notice that, by Proposition 1.6, problem (5) is equivalent to

$$\begin{aligned} \min \ \Big\{ \int_F \big(\mathrm{div}_\tau \ \xi\big)^2 \ \mathrm{d}\mathcal{H}^2(x) : \ \xi \in L^\infty(F; \mathbb{R}^3), \ \mathrm{div}_\tau \ \xi \in L^2(F), \\ \xi \in T^o(\nabla d_\phi^E) \ \mathcal{H}^2 - a.e. \text{ in } F, \ \xi \cdot \nu_F = c_F \text{ on } \partial F \Big\}. \end{aligned} \tag{6}$$

for any facet $F \subset \partial E$.

We fix a facet $F \subset \partial E$ and we assume that $\partial E(t)$ is the graph of a Lipschitz continuous function $u : \Omega \times [0,\tau] \to \mathbb{R}$, in a neighbourhood of F. Let P be the projection of F on Ω. Then equation (3) becomes

$$\begin{cases} u_t \in -\phi^o(-\nabla u, 1) \ \partial^- \Phi(u), & \text{a.e. } (x,t) \in \Omega \times [0,\tau], \\ u(x,0) = u_0(x), & x \in \Omega, \\ u(x,t) = v(x,t), & (x,t) \in \partial\Omega \times [0,\tau], \end{cases} \tag{7}$$

where $u_0 \in \mathrm{Lip}(\Omega)$ represents the set ∂E as graph over Ω, $v(\cdot,t) \in \mathrm{Lip}(\partial\Omega)$, $t \in [0,\tau]$, represents the set $\partial E(t)$ as a graph over $\partial\Omega$ and $\Phi : H^1(\Omega) \subset L^2(\Omega) \to \mathbb{R}$ is defined as

$$\Phi(u) := \int_\Omega \phi^o(-\nabla u, 1) \ \mathrm{d}x.$$

Here ∂^- is the subdifferential in $L^2(\Omega)$ in the sense of convex analysis [9].

By [9, Lemma 9.1], there holds

$$f \in \partial^- \Phi(u) \iff f = \operatorname{div} \eta,$$

for some $\eta \in \left[L^1_{\mathrm{loc}}(\Omega)\right]^2$, with $\eta \in \partial^- \phi^o(-\nabla u, 1)$ a.e. in Ω. Notice that this constraint on η implies that $\eta \in \left[L^\infty(\Omega)\right]^2$.

On the analogy of the results discussed in [6] for maximal monotone operators, we can expect that $u_t = -\big(\phi^o(-\nabla u, 1)\ \partial^- \Phi(u)\big)^0$ for a.e. $t \in [0, \tau]$, where $\big(\phi^o(-\nabla u, 1)\ \partial^- \Phi(u)\big)^0$ solves

$$\min \big\{ ||\phi^o(-\nabla u, 1)\ f||_{L^2(\Omega)} :\ f \in \partial^- \Phi(u) \big\}, \tag{8}$$

which in turn gives (5).

The following result (see [4]) is useful in order to characterize which facets of ∂E do not break during the evolution.

Proposition 1.7. *Let (E, n_ϕ) be a ϕ-regular pair. Assume that E is a polyhedron and let F be a facet of ∂E. If F does not instantly break or bend during the evolution starting from E, then the following condition holds:*

$$v_P := |P|^{-1} \int_{\partial P} c_P(s)\ \mathrm{d}\mathcal{H}^1(s) \geq v_F, \tag{9}$$

for any set $P \subseteq F$ with Lipschitz continuous boundary, where

$$c_P(s) := \begin{cases} c_F(s) & \text{if } s \in \partial P \cap \partial F, \\ \sup\ \{n \cdot \nu_P(s) :\ n \in T^o(\nabla d^E_\phi)\} & \text{otherwise.} \end{cases}$$

Proof. From (3) we have $\kappa_\phi(x) = v_F$ for any $x \in F$. Moreover, if we integrate κ_ϕ over P, we get

$$|P| v_F = \int_P \kappa_\phi(x)\ \mathrm{d}\mathcal{H}^2(x) = \int_{\partial P} n_\phi(s) \cdot \nu_P(s)\ \mathrm{d}\mathcal{H}^1(s) \leq \int_{\partial P} c_P(s)\ \mathrm{d}\mathcal{H}^1(s),$$

which implies (9). □

We expect that condition (9) is also sufficient for a facet $F \subset \partial E$ not to break during the evolution.

2. The algorithm

In order to give numerical examples of facet–breaking, we consider a single polygonal facet $F \subset \partial E$ (we shall consider F as a subset of $\mathbb{R}^2$) and minimize the functional

$$\mathcal{E}_\phi(\xi) := \int_F (\mathrm{div}\ \xi(x))^2\ \mathrm{d}x, \tag{10}$$

over all functions $\xi \in L^\infty(F;\mathbb{R}^2)$ such that $\mathrm{div}\ \xi \in L^2(F)$, $\xi \cdot \nu_F = c_F$ assigned, and $\xi \in W$ a.e. in F, where W is the orthogonal projection on the plane containing F of the convex set $T^o(\nabla d^E_{\phi\,|F})$.

We observe that, following [9, Section 9.c], the functional (10) admits a minimum $\xi_{\min} \in L^\infty(F;\mathbb{R}^2)$ under the previous restrictions; moreover two different minima of (10) have the same divergence in F.

By (6), we expect that if ξ is a minimum of (10) then $-\mathrm{div}\ \xi$ represents the velocity (along the Cahn-Hoffman vector field) of the points of F, so that possible fractures will appear in correspondance of discontinuities of $\mathrm{div}\ \xi$ while, if $\mathrm{div}\ \xi$ is continuous but non constant, the facet F will bend.

Here is a brief explanation of the numerical algorithm used to find the minima of (10). We use a finite element method: given a triangulation of F with vertices $x_1, \ldots, x_N$, we consider the finite dimensional space of piecewise linear functions

$$\xi = \sum_{i=1}^N \xi_i \phi_i,$$

with $\xi_i \in \mathbb{R}^2$ and $\phi_i : F \to \mathbb{R}$ being continuous functions which are linear on every single triangle and such that $\phi_i(x_j) = \delta_{ij}$ (hat functions). It is not difficult to find the gradient of the functional (10) restricted to this space of functions:

$$\frac{\partial \mathcal{E}_\phi}{\partial \xi_i}(\xi) = \sum_j M_{ij}\xi_j, \tag{11}$$

where M_{ij} are the 2×2 matrices given by

$$M_{ij} = 2\int_F \nabla\phi_i \otimes \nabla\phi_j\ \mathrm{d}x.$$

Given a triangulation of F and an initial admissible guess ξ, we look for a minimum of $\mathcal{E}_\phi$ letting ξ evolve following (minus) the gradient of $\mathcal{E}_\phi$ given by (11). After each step of the evolution, we project ξ onto the constraint W, in order to guarantee that ξ is always admissible for (10).

We begin with a huge triangulation of F and, as initial guess, we consider $\xi := c_F \ \nu_F$ on ∂F and $\xi := 0$ inside F. Then we compute the matrix M_{ij} and we start the steepest descent minimizing evolution for $\mathcal{E}_\phi$. When we are close enough to a minimum of $\mathcal{E}_\phi$ for the given triangulation we thicken the triangulation by adding new triangles where div ξ has more variation, and then we restart the minimization process with the new triangulation and the new initial guess.

3. Examples and conclusions

In this section we show the numerical results obtained in two simple examples for which it is possible to find explicitly the velocity field (see [4], [13]).

In the first example we consider the crystalline norm on $\mathbb{R}^3$ given by $\phi(x) := \max\{|x_1|, |x_2|, |x_3|\}$, and we let $E := F \times [0,1]$, where F is a non convex polygon which is the union of a square and a rectangle, see Figure 1.

In Figure 1 it is shown the adaptive triangulation constructed by the alghorithm during the minimization process. We notice that small triangles are created along the segment separating the square from the rectangle, where the velocity has a great oscillation. In Figure 2 the contour curves of the resulting velocity are shown. We notice that on the segment between the square and the rectangle the contour curves accumulate, while elsewhere the resulting normal velocity is nearly constant. This is in agreement with the theoretical result predicting the fracture of F along the segment [4].

In the second example we consider a crystalline norm whose Wulff shape is an orthogonal prism centered at the origin, having a regular hexagon as basis. We let $E := F \times [0,1]$, where F is the hexagon shown in Figure 3.

We notice that the computed velocity has great oscillations in correspondance of the short edges of F. More precisely, the velocity seems to increase approaching such edges. In Figure 4 the contour curves of the resulting velocity are shown. Indeed, by the argument discussed

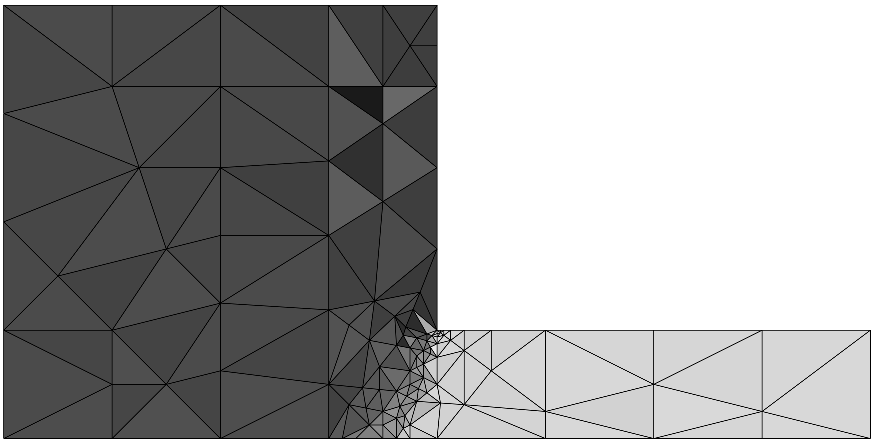

Figure 1: The adaptive triangulation. The brightness of colors represents the value of div ξ on every triangle.

in [4], one expects that the velocity is continuous on F (increasing near the short edges), so that the facet F should bend inside E during the evolution.

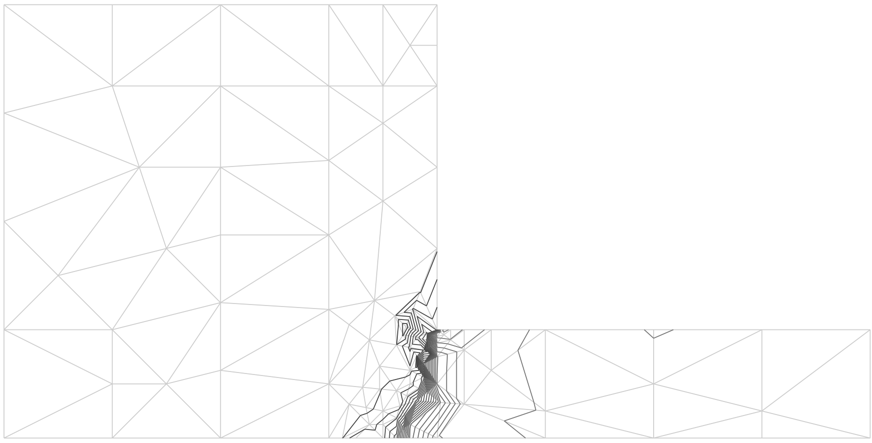

Figure 2: The contour curves of div ξ

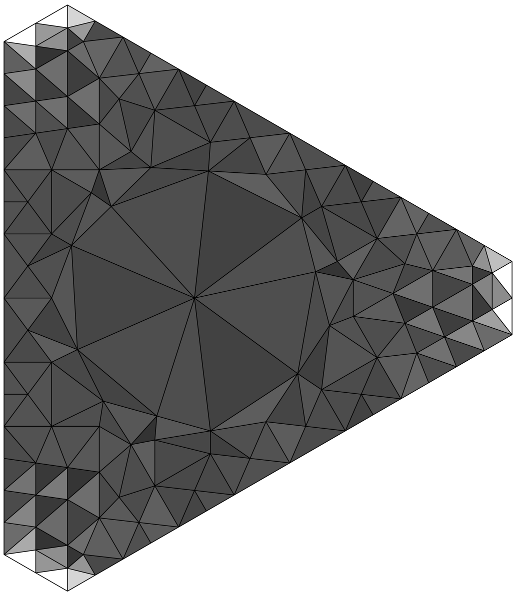

Figure 3: The adaptive triangulation. The brightness of colors represents the value of div ξ on every triangle.

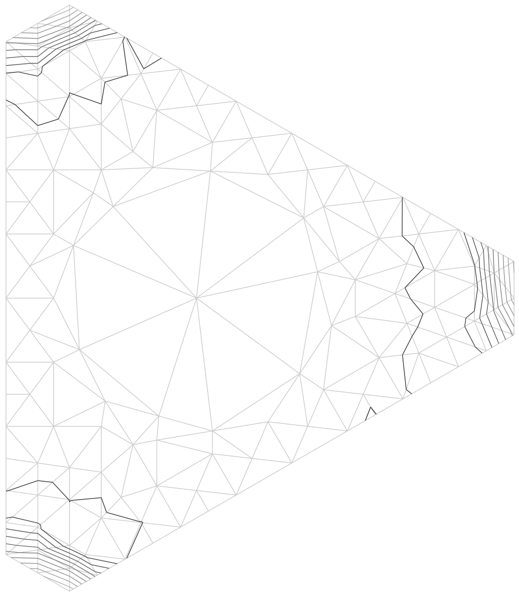

Figure 4: The contour curves of div ξ

References

[1] F.J. Almgren and J. Taylor. Flat flow is motion by crystalline curvature for curves with crystalline energies. *J. Diff. Geom.*, 42:1–22, 1995.

[2] F.J. Almgren, J.E. Taylor, and L. Wang. Curvature-driven flows: a variational approach. *SIAM J. Control Optim.*, 31:387–437, 1993.

[3] G. Bellettini and M. Novaga. Approximation and comparison for non-smooth anisotropic motion by mean curvature in $\mathbf{R^N}$. *Math. Mod. Meth. Appl. Sc.*, (to appear).

[4] G. Bellettini, M. Novaga, and M. Paolini. Facet-breaking for three-dimensional crystals evolving by mean curvature. *Interfaces and Free Boundaries*, (to appear).

[5] G. Bellettini, M. Paolini, and S. Venturini. Some results on surface measures in Calculus of Variations. *Ann. Mat. Pura Appl.*, 170:329–359, 1996.

[6] H. Brezis. *Operateurs Maximaux Monotones.* North-Holland, Amsterdam, 1973.

[7] J.W. Cahn, C.A. Handwerker, and J.E.Taylor. Geometric models of crystal growth. *Acta Metall. Mater.*, 40:1443–1474, 1992.

[8] M.-H. Giga and Y. Giga. A subdifferential interpretation of crystalline motion under nonuniform driving force. *Dynamical Systems and Differential Equations*, 1:276–287, 1998.

[9] Y. Giga, M.E. Gurtin, and J. Matias. On the dynamics of crystalline motion. *Japan Journal of Industrial and Applied Mathematics*, 15:7–50, 1998.

[10] J.E. Taylor. Crystalline variational problems. *Bull. Amer. Math. Soc. (N.S.)*, 84:568–588, 1978.

[11] J.E. Taylor. Geometric crystal growth in 3D via facetted interfaces. *In: Computational Crystal Growers Workshop, Selected Lectures in Mathematics, Amer. Math. Soc.*, pages 111–113, 1992.

[12] J.E. Taylor. Mean curvature and weighted mean curvature. *Acta Metall. Mater.*, 40:1475–1485, 1992.

[13] J. Yunger. Facet Stepping and Motion By Crystalline Curvature. *PhD Thesis*, 1998.

M. Novaga, E. Paolini: Scuola Normale Superiore, Piazza dei Cavalieri 7, 56126 Pisa.